THE SOUTH POLAR REGION AS SEEN BY THE LUNAR ORBITER LASER ALTIMETER (LOLA)

Michael K. Barker[1], Erwan Mazarico[1], Gregory A. Neumann[1], David E. Smith[2], Maria T. Zuber[2] and James W. Head[3], [1]NASA Goddard Space Flight Center, Greenbelt, MD 20771, USA, [2]Department of Earth, Atmospheric, and Planetary Sciences, MIT, Cambridge, MA, 02139, USA, [3]Department of Earth, Environmental and Planetary Sciences, Brown University, Providence, RI 02912, USA

Introduction: Precise and accurate topographic maps, and their derived products, are critical inputs to many aspects of mission design, including landing site selection [1]. We need to know the topography on a variety of scales to fully characterize candidate landing sites locally and regionally. Laser altimeters, such as the Lunar Orbiter Laser Altimeter (LOLA) on the Lunar Reconnaissance Orbiter (LRO), have the advantage of seeing into shadows given their active ranging capabilities. The LOLA altimetric dataset provides the geodetic framework with which all other lunar datasets can locate their data to within ~10 m horizontally and ~1 m vertically [2]. LOLA data products also inform landing site selection by providing surface height, slope, roughness (Figure 1), reflectance, and illumination (Figure 2). Here we provide a specific example of how LOLA topographic data can inform the broader geologic context [8] of the Artemis III candidate sites.

Roughness: A variety of surface processes operate over a wide range of horizontal scales to shape the lunar landscape over time [e.g., 3–6]. Therefore, topographic roughness can provide valuable information on landscape evolution and geologic history. We make roughness maps by computing an outlier-resistant standard deviation of height residuals for individual LOLA spots relative to a plane fit over different baselines. It is helpful to visualize the roughness at multiple baselines combined into a color composite image (Figure 1). A strong intensity of a particular color signifies a relatively high roughness at the corresponding baseline.

This map reveals a diversity of terrains characterized by their "roughness spectrum." Some areas, such as the floors of Amundsen and Newton A, appear blue to cyan signifying a pronounced increase in roughness at baselines < 400 m relative to 800 – 1600 m. These regions are relatively heavily populated with craters of diameter < 400 m. Several linear features are apparent, extending predominantly up-down (in plan view). These are most visible at baselines < 400 m with shades of blue to cyan. The thinnest of these (A – C in Figure 1) have widths < 5 km and may be examples of the "roughness rays and lineaments" previously identified at lower latitudes in global hectometer-scale roughness maps and which may be chains of secondary craters [4]. There is also tentative evidence for two additional diffuse, longer, and wider swaths (D and E) of variably high roughness on short baselines. Swath D may be part of a Tycho ejecta ray [7,8]. If E is another ejecta ray, then that could explain why Amundsen's floor is so rough at short baselines compared to other large craters. Non-uniformities in swath width and roughness could reflect variations in density of secondary impactors and/or target terrain properties.

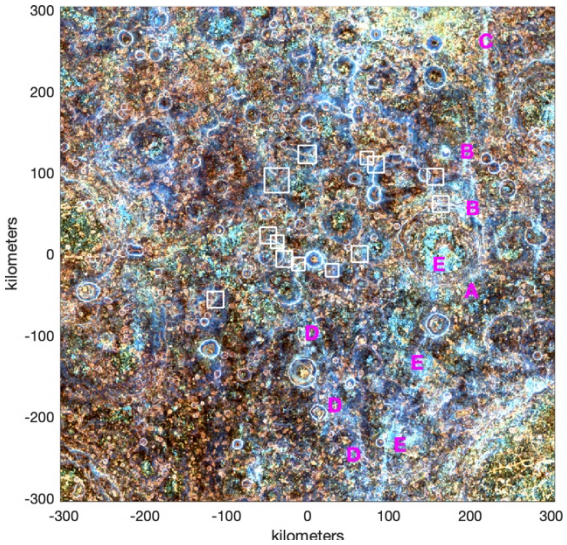

Figure 1 – Color composite image of LOLA surface roughness with each baseline assigned to a different color: 50 m (blue), 100 m (teal), 200 m (cyan), 400 m (yellow), 800 m (orange) and 1600 m (red).

Altogether, this view of the south polar region highlights the role that even far-away impacts can have in shaping the terrain and redistributing material. The distribution of ejecta can be mapped, in part, by LOLA roughness. One implication for site selection is that secondary ejecta should be considered when interpreting sample provenance [9] and other in-situ data.

References: [1] Heldmann, J. L., et al., 2016, Acta Astron., 127, 308. 10.1016/j.actaastro.2016.06 .014. [2] Smith, D. E., et al. 2017, Icarus, 283, 70. 10.1016/j .icarus.2016.06.006. [3] Deutsch, A., et al., 2021, PSJ, 2, 213. 10.3847/PSJ/ac24ff. [4] Kreslavsky, M. A., et al., 2013, Icarus, 226, 52. 10.1016/j.icarus.2013.04 .027. [5] Wang, J., et al., 2020, JGRE, 125, 10, e06091 .10.1029/2019JE006091. [6] Cai, Y. & Fa, W., 2020, JGRE, 125, 8. 10.1029/2020JE006429. [7] Bernhardt H., et al., 2022, Icarus, 379, 114963. 10.1016/ j.icarus.2022.114963. [8] Denevi, B. W., et al, this conference. [9] Krasilnikov, S. S., et al., 2023, Icarus, 394, 115422. 10.1016/j.icarus.2022.115422.

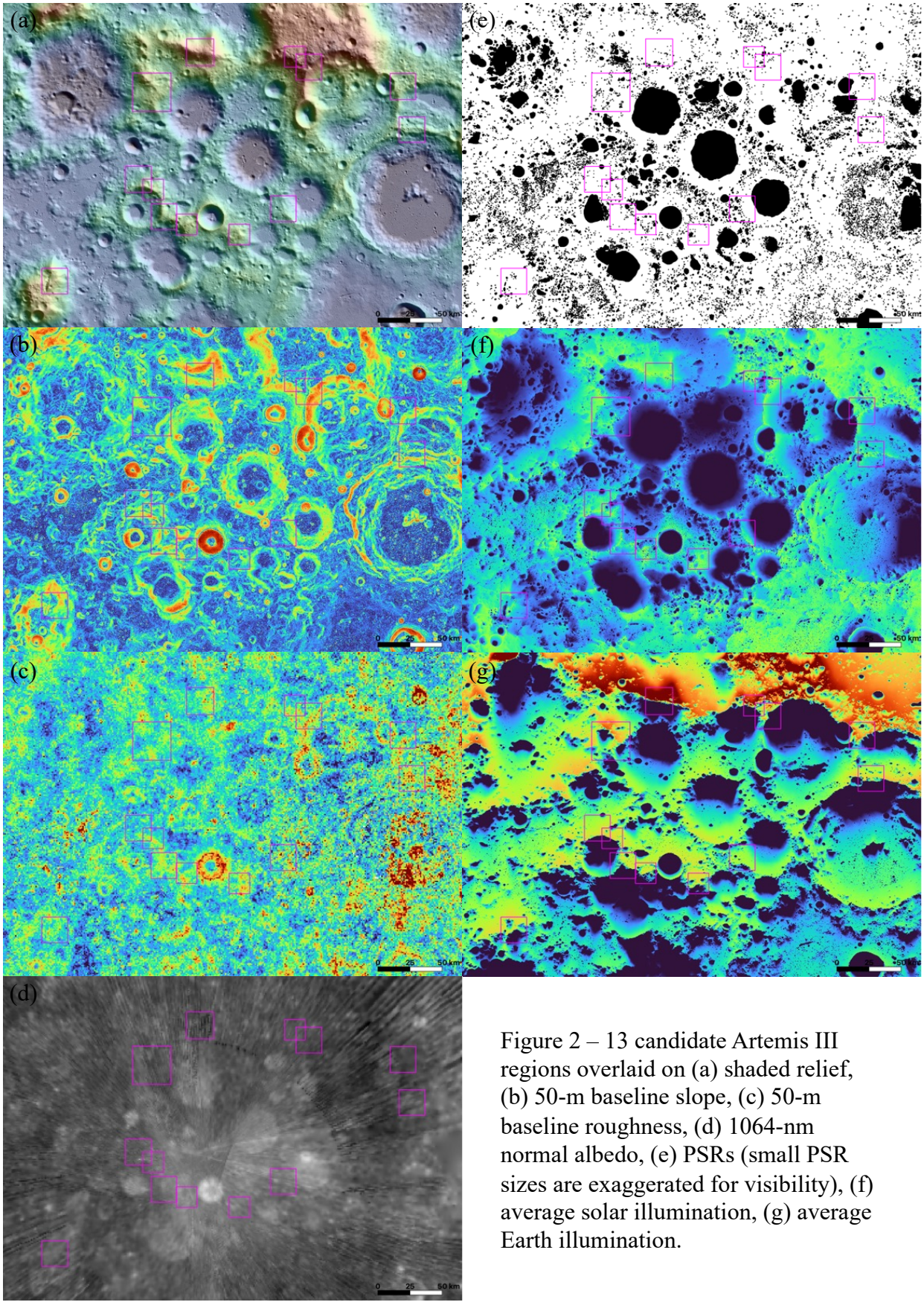

Figure 2 – 13 candidate Artemis III regions overlaid on (a) shaded relief, (b) 50-m baseline slope, (c) 50-m baseline roughness, (d) 1064-nm normal albedo, (e) PSRs (small PSR sizes are exaggerated for visibility), (f) average solar illumination, (g) average Earth illumination.